



Description of Elastic Forces in Absolute Nodal Coordinate Formulation

JUSSI T. SOPANEN and AKI M. MIKKOLA

Department of Mechanical Engineering, Lappeenranta University of Technology, Skinnarilankatu 34, SF-53851 Lappeenranta, Finland; E-mail: {jsopanen, mikkola}@lut.fi

(Received: 24 January 2003; accepted: 24 April 2003)

Abstract. The objective of this paper is to investigate the accuracy of the elastic force models that can be used in the absolute nodal coordinate finite element formulation. This study focuses on the description of the elastic forces in three-dimensional beams. The elastic forces of the absolute nodal coordinate formulation can be derived using a continuum mechanics approach. This study investigates the accuracy and usability of such an approach for a three-dimensional absolute nodal coordinate beam element. This study also presents an improvement proposal for the use of a continuum mechanics approach in deriving the expression of the elastic forces in the beam element. The improvement proposal is verified using several numerical examples that show that the proposed elastic force model of the beam element agrees with the analytical results as well as with the solutions obtained using existing finite element formulation. In the beam element under investigation, global displacements and slopes are used as the nodal coordinates, which resulted in a large number of nodal degrees of freedom. This study provides a physical interpretation of the nodal coordinates used in the absolute nodal coordinate beam element. It is shown that a beam element based on the absolute nodal coordinate formulation relaxes the assumption of a rigid cross-section and is capable of representing a distortional deformation of the cross-section. The numerical results also imply that the beam element does not suffer from the phenomenon called shear locking.

Keywords: Finite element formulations, beams, elastic forces, continuum mechanics.

1. Introduction

Multibody simulation has been proven to be an effective tool for the design of machines. With the help of multibody simulation, some physical prototypes can be avoided and, in this way, the product development cycle speeded up. The multibody simulation approach is based on the concept of replacing an actual system with an equivalent mathematical model that consists of discrete bodies. This concept is useful when the bodies are either rigid or linearly deformable. Consequently, multibody simulation can be used to analyze a wide variety of machines including robots, vehicles, manipulators and mechanisms. Multibody simulation has recently been extended to cases in which a body exhibits nonlinear deformation. This important generalization makes it possible to build more accurate and sophisticated simulation models. Nonlinear deformation should be considered when, for example, cables, belts and slender robot arms are under investigation. Nonlinear deformation can be taken into account in multibody simulations through the use of, for example, the large rotation vector formulation or the absolute nodal coordinate formulation.

In the large rotation vector formulation [1–9], the rotations of the cross-section and global displacements of the centerline of an element are used as the nodal coordinates. The cross-section rotation within an element is approximated through the use of interpolation polynomials. The finite element interpolation of the rotations must be carefully handled, since it

can lead to frame-indifferent and path-dependent elements, as described in [8]. Moreover, the use of rotations as the nodal coordinates often leads to excessive shear forces, which produces a phenomenon known as shear locking. This problem can be alleviated using a reduced numerical integration procedure. In some cases, reduced numerical integration can produce an ill-conditioned stiffness matrix, which leads to spurious zero energy modes. In the large rotation vector formulation, the rigid body motion and deformation of the beam element are expressed directly in a fixed inertial frame. This simplifies the description of the inertia of the element. It is important to note, however, that, in a three-dimensional case, the large rotation vector formulation does not lead to a constant mass matrix.

The absolute nodal coordinate formulation is a recently developed method based on finite element formulation [10] and is designed for large deformation multibody analysis; the absolute nodal coordinate formulation has been successfully applied to three-dimensional beams [11, 12] and shells [13]. In the absolute nodal coordinate formulation, slopes and displacements are used as the nodal coordinates instead of infinitesimal or finite rotations. This helps avoid the cumbersome interpolation of rotational coordinates. By using slopes instead of rotations, no assumptions are made with regard to the magnitude of the deformation within the element. The formulation can be used systematically to relax some of the assumptions used in classical beam and plate models [12, 13]. The absolute nodal coordinate formulation uses a displacement field that is linear in the nodal coordinates. In addition, the shape function matrix, together with the nodal coordinates, is able to describe arbitrary rigid body motion. For these reasons, the absolute nodal coordinate formulation leads to a constant mass matrix in two- and three-dimensional cases. The constant mass matrix simplifies the nonlinear equations of motion and, consequently, accelerates the time integration of the nonlinear equations of motion. The absolute nodal coordinate formulation can be used in the framework of a non-incremental solution procedure.

The objective of this study is to investigate the kinematics, as well as the stiffness properties, of the absolute nodal coordinate formulation. This is accomplished by comparing the absolute nodal coordinate formulation with the large rotation vector formulation in static cases. This study focuses particularly on a three-dimensional beam element that is based on the use of the absolute nodal coordinate formulation. The beam element was originally proposed by Shabana and Yakoub [11] and is capable of representing large deformations and arbitrary rigid body motion. As demonstrated by Yakoub and Shabana [12], the elastic forces of the beam element can be derived using a continuum mechanics approach. This study discusses the accuracy and usability of such an approach. This study proposes an improvement to the expression of the elastic forces of the beam element. The three-dimensional beam element, based on the absolute nodal coordinate formulation, uses slopes and displacements as the nodal coordinates, which leads to a large number of generalized coordinates. This study offers a physical interpretation of the nodal degrees of freedom used in the beam element. By using the absolute nodal coordinate formulation, it is possible to obtain an expression for the elastic forces, which takes into account the effect of shear deformation. This paper also discusses the accuracy of the shear forces of the absolute nodal coordinate beam element.

2. The Large Rotation Vector Formulation

The large rotation vector formulation [1–9] is based on the large displacement and rotation theory. In this formulation, a vector field defines the position of the centerline of the ele-

ment. The cross-section of the beam is defined by a moving frame, which is oriented by an orthogonal matrix, i.e. a rotation matrix. In the large rotation vector formulation, it is assumed that the cross-section remains plane and maintains its area, as well as its shape, during deformation. This formulation expresses rigid body motion and the deformation of the beam element directly in the fixed inertial frame. The configuration of the beam is described completely by vector \mathbf{R} that defines the centerline of the beam and the rotation matrix, $\mathbf{\Lambda}$, as follows:

$$\mathbf{r}(x, y, z) = \mathbf{R}(x) + \mathbf{\Lambda}(x) \begin{bmatrix} 0 \\ y \\ z \end{bmatrix}, \quad (1)$$

where x is a coordinate along the centerline of the beam and y and z are coordinates on the cross-section. The rotation matrix can be parameterized by using the rotational vector as follows [7]

$$\mathbf{\Lambda} = \exp \tilde{\boldsymbol{\psi}} = \mathbf{I} + \frac{\sin \psi}{\psi} \tilde{\boldsymbol{\psi}} + \frac{1 - \cos \psi}{\psi^2} \tilde{\boldsymbol{\psi}}^2, \quad (2)$$

where $\tilde{\boldsymbol{\psi}}$ is the skew-symmetric matrix associated with the rotational vector $\boldsymbol{\psi} = [\psi_1 \ \psi_2 \ \psi_3]^T$ and $\psi = \sqrt{\psi_1^2 + \psi_2^2 + \psi_3^2}$.

During the solution procedure, the rotation matrix must be updated. The relationship between the rotation matrices in two consecutive configurations, k and $k + 1$, of the element can be defined using the rotational vector as follows:

$$\mathbf{\Lambda}^{k+1} = \exp \tilde{\boldsymbol{\psi}} \mathbf{\Lambda}^k. \quad (3)$$

In the large rotation vector formulation, strains are defined through the use of a body-attached frame. This can be accomplished by defining translational $\boldsymbol{\Gamma}$ and rotational $\boldsymbol{\kappa}$ strain measures using the current configuration of the beam element, $(\mathbf{R}, \mathbf{\Lambda})$, as follows:

$$\boldsymbol{\Gamma} = \mathbf{\Lambda}^T \mathbf{R}' - \begin{bmatrix} 1 \\ 0 \\ 0 \end{bmatrix}, \quad (4)$$

$$\boldsymbol{\kappa} = \mathbf{\Lambda}^T \boldsymbol{\omega}, \quad (5)$$

where the vector $\boldsymbol{\omega}$ can be obtained by employing the rotational vector. In Equation (4), \mathbf{R}' is a derivation of vector \mathbf{R} with respect to x . In the large rotation vector formulation, it is difficult to establish the relationship between finite rotations and strains [7]. The representation of the three-dimensional rotation of a moving frame with respect to the inertial frame is not linear, while the finite rotations are, in general, not commutative. The interpolation of the rotations along the beam length becomes, thus, nontrivial and must be handled carefully. As pointed out by Jelenić and Crisfield [8], the interpolation of the rotation coordinates of the beam element can lead to frame-indifferent and path-dependent elements. In the large rotation vector formulation, the strain measures may not be invariant under rigid body motion and the strains may be dependent on the history of the deformation. In order to overcome these drawbacks, Jelenić and Crisfield [8] proposed the interpolation of local rotations in a co-rotational manner.

Another approach for three-dimensional beam formulation was proposed by Avello and García de Jalón [4]. They used orthogonal unit vectors to describe the cross-section of the

beam. The components of these vectors are used as nodal variables, and finite element interpolation is applied to these vectors instead of to the rotational degrees of freedom. Constraint equations are used to obtain orthonormality and the unit length conditions of the vectors that define the cross-section of the beam. This method causes the mass matrix of the beam element to become constant and singular. It must be noted that the singularity of the mass matrix is not a problem, since the equations of motion are solved using the Newmark procedure, which does not require the inverse of the mass matrix.

3. The Kinematics of Absolute Nodal Coordinate Formulation

3.1. THE KINEMATICS OF AN ELEMENT

In the absolute nodal coordinate formulation, the global position vector, \mathbf{r} , of an arbitrary point on a three-dimensional element can be written as

$$\mathbf{r} = \mathbf{S}(x, y, z)\mathbf{e}, \quad (6)$$

where \mathbf{S} is the element shape function matrix, x , y and z are the local coordinates of the element and \mathbf{e} is the vector of the nodal coordinates. The shape function matrix and vector of the nodal coordinates must be selected in such a way that they represent both arbitrary rigid body motion and element deformation. The displacement field of a three-dimensional beam element can be obtained using the following polynomial expression [12]:

$$\mathbf{r} = \begin{bmatrix} r_1 \\ r_2 \\ r_3 \end{bmatrix} = \begin{bmatrix} a_0 + a_1x + a_2y + a_3z + a_4xy + a_5xz + a_6x^2 + a_7x^3 \\ b_0 + b_1x + b_2y + b_3z + b_4xy + b_5xz + b_6x^2 + b_7x^3 \\ c_0 + c_1x + c_2y + c_3z + c_4xy + c_5xz + c_6x^2 + c_7x^3 \end{bmatrix}. \quad (7)$$

In Equation (7), the element is described as being a continuous volume, which makes the deformation of the cross-section possible. The assumed displacement field in Equation (7) includes 24 unknown polynomial coefficients. For a two-noded beam element (I, J), 12 nodal coordinates can be used for each node. The coordinates of node I , \mathbf{e}_I , can be written as

$$\mathbf{e}_I = \begin{bmatrix} \mathbf{r}_I^T & \frac{\partial \mathbf{r}_I^T}{\partial x} & \frac{\partial \mathbf{r}_I^T}{\partial y} & \frac{\partial \mathbf{r}_I^T}{\partial z} \end{bmatrix}^T, \quad (8)$$

where vector \mathbf{r}_I defines the global position of node I and vectors $\partial \mathbf{r}_I / \partial x$, $\partial \mathbf{r}_I / \partial y$ and $\partial \mathbf{r}_I / \partial z$ are the slopes at node I . Using the interpolating polynomial introduced in Equation (7) and the nodal coordinates, the element shape function matrix, \mathbf{S} , can be expressed as follows:

$$\mathbf{S} = [S_1\mathbf{I} \ S_2\mathbf{I} \ S_3\mathbf{I} \ S_4\mathbf{I} \ S_5\mathbf{I} \ S_6\mathbf{I} \ S_7\mathbf{I} \ S_8\mathbf{I}], \quad (9)$$

where \mathbf{I} is a 3×3 identity matrix and

$$S_1 = 1 - 3\xi^2 + 2\xi^3, \quad S_2 = l(\xi - 2\xi^2 + \xi^3), \quad S_3 = l\eta(1 - \xi), \quad S_4 = l\zeta(1 - \zeta), \\ S_5 = 3\xi^2 - 2\xi^3, \quad S_6 = l(-\xi^2 + \xi^3), \quad S_7 = l\xi\eta, \quad S_8 = l\xi\zeta.$$

The non-dimensional quantities, ξ , η , ζ , are defined as

$$\xi = \frac{x}{l}, \quad \eta = \frac{y}{l}, \quad \zeta = \frac{z}{l},$$

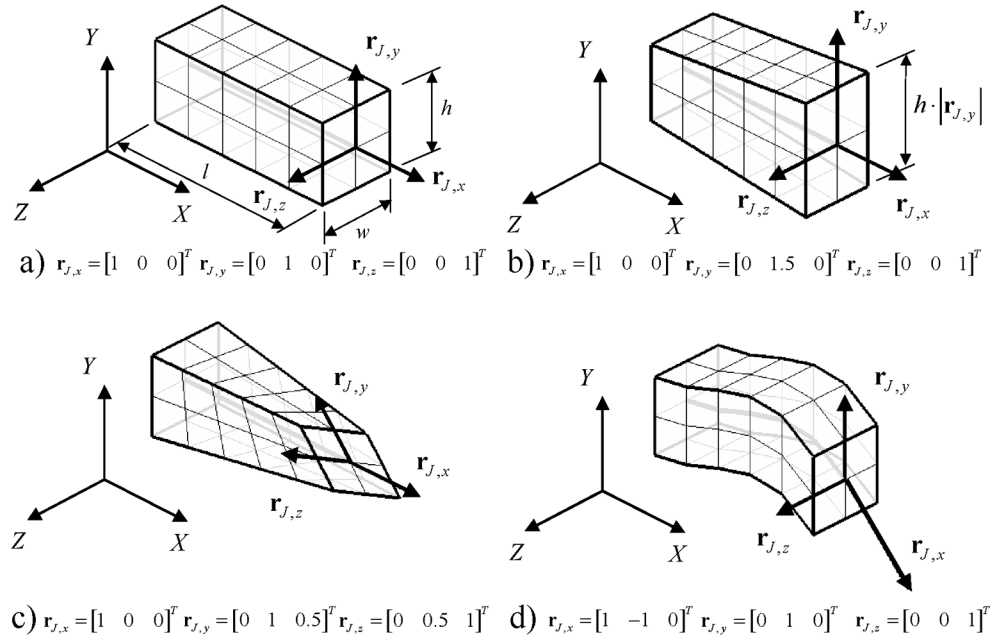


Figure 1. The physical interpretation of the slope coordinates.

where l is the length of the beam element in the initial configuration.

3.2. THE PHYSICAL INTERPRETATION OF THE SLOPE COORDINATES

In the beam element introduced above, the 24 nodal coordinates are independent. Physically, this means that the cross-section of the beam can deform. In general, vector $\partial \mathbf{r} / \partial x$ defines the global orientation of the centerline of the beam. Correspondingly, the orientation of the height and the width coordinates of the cross-section of the beam are defined by vectors $\partial \mathbf{r} / \partial y$ and $\partial \mathbf{r} / \partial z$. The length deviation of these vectors from unity describes the elongation or contraction in the corresponding direction. To illustrate this, we consider the simple prismatic beam shown in Figure 1. For simplicity, the beam is initially parallel to the global coordinate system. Vectors $\mathbf{r}_{J,x} = \partial \mathbf{r}_J / \partial x$, $\mathbf{r}_{J,y} = \partial \mathbf{r}_J / \partial y$ and $\mathbf{r}_{J,z} = \partial \mathbf{r}_J / \partial z$ are the slope coordinates at node J . In Figure 1a, these vectors are orthogonal unit vectors. This is a special case in which the cross-section of the beam is normal to the beam's centerline. In Figure 1b, the vectors are still orthogonal but the length of vector $\mathbf{r}_{J,y}$ has increased from unity. As a result, the height of the cross-section increases. In Figure 1c, vectors $\mathbf{r}_{J,y}$ and $\mathbf{r}_{J,z}$ are not orthogonal unit vectors, and the resulting deformed shape of the beam represents the distortional deformation of the cross-section. In Figure 1d, vector $\mathbf{r}_{J,x}$ is modified; for this reason, the orientation and length of the centerline of the beam at node J has changed. Figure 1 shows that a beam element, based on the absolute nodal coordinate formulation, relaxes the assumption of a rigid cross-section. The slope coordinates can describe the shearing, axial, transverse, torsion and distortional deformation of the element. The values of the slope coordinates at any arbitrary point on the element can be interpolated with the use of nodal coordinates. The interpolation of the slope coordinates, unlike that of infinite or finite rotations, is straightforward.

4. Description of Externally Applied Loads

4.1. EXTERNAL FORCE

The principle of virtual work can be used to develop the vector of the generalized forces [10]. The virtual work caused by the external force vector acting on an arbitrary point on the element can be written as

$$\delta W = \mathbf{F}^T \delta \mathbf{r} = \mathbf{F}^T \mathbf{S} \delta \mathbf{e} = \mathbf{Q}_f^T \delta \mathbf{e}, \quad (10)$$

where \mathbf{r} is the position vector of the point of the applied force and $\mathbf{Q}_f = \mathbf{S}^T \mathbf{F}$ the vector of the generalized forces associated with the nodal coordinates. The virtual work caused by distributed forces, such as gravity forces, can be obtained by integrating Equation (10) over the volume of the element [16].

4.2. EXTERNAL MOMENT

In the absolute nodal coordinate formulation, the external moments are functions of the nodal coordinates. This is because slopes, instead of rotations, are used to define the orientation of the element. As shown earlier, the slope vectors define the orientation of the cross-section of the beam. On the other hand, externally applied moments change the orientation of the cross-section. Thus, the externally applied moments must be described as forces that affect the components of the slope vectors. The generalized external forces caused by the applied moments can be defined with the help of virtual work [16]. For the sake of simplicity, the following equations are derived by assuming that the element is initially parallel to the global coordinate system. The virtual work caused by externally applied moments around the x -, y - and z -axis is given by

$$\delta W_M = \mathbf{M}^T \delta \boldsymbol{\gamma}, \quad (11)$$

where

$$\mathbf{M} = [M_x \ M_y \ M_z]^T, \quad (12)$$

$$\boldsymbol{\gamma} = [\gamma_x \ \gamma_y \ \gamma_z]. \quad (13)$$

The positive directions of the applied moments, M_x , M_y and M_z , around the x -, y - and z -axis of the beam are determined by the right-hand rule. Vector $\boldsymbol{\gamma}$ contains the rotation angles of the vectors that define the cross-section. The virtual changes in these angles can be defined by using the slope coordinates [16]. The virtual change in the orientation angle of the cross-section around the z -axis of the beam can be defined as

$$\delta \gamma_z = \frac{-(\partial r_2 / \partial y) \delta (\partial r_1 / \partial y) + (\partial r_1 / \partial y) \delta (\partial r_2 / \partial y)}{d_{yx}}, \quad d_{yx} = \left(\frac{\partial r_1}{\partial y} \right)^2 + \left(\frac{\partial r_2}{\partial y} \right)^2. \quad (14)$$

Correspondingly, the virtual change in the orientation angle of the cross-section around the y -axis of the beam can be written as

$$\delta \gamma_y = \frac{(\partial r_3 / \partial z) \delta (\partial r_1 / \partial z) - (\partial r_1 / \partial z) \delta (\partial r_3 / \partial z)}{d_{zx}}, \quad d_{zx} = \left(\frac{\partial r_1}{\partial z} \right)^2 + \left(\frac{\partial r_3}{\partial z} \right)^2. \quad (15)$$

The virtual change in the orientation angle of the cross-section around the x -axis can be written as

$$\delta\gamma_x = \frac{(\partial r_2/\partial y)\delta(\partial r_3/\partial y) - (\partial r_3/\partial y)\delta(\partial r_2/\partial y)}{d_{yz}} + \frac{(\partial r_2/\partial z)\delta(\partial r_3/\partial z) - (\partial r_3/\partial z)\delta(\partial r_2/\partial z)}{d_{zy}}, \quad (16)$$

where

$$d_{yz} = \left(\frac{\partial r_2}{\partial y}\right)^2 + \left(\frac{\partial r_3}{\partial y}\right)^2, \quad d_{zy} = \left(\frac{\partial r_2}{\partial z}\right)^2 + \left(\frac{\partial r_3}{\partial z}\right)^2. \quad (17)$$

It can be seen from Equation (16) that the torsion moment is applied to two vectors, and thus, moment M_x must be distributed evenly among them. The slope coordinates can be interpolated using the nodal coordinates and shape function matrix. If an external torsion moment, M_x , acts on node I of the beam element, the generalized external force vector applied on node I can be written as follows:

$$\mathbf{Q}'_f = \frac{M_x}{2} \begin{bmatrix} 0 & 0 & 0 & 0 & 0 & 0 & 0 & -\frac{e_9}{d'_{yz}} & \frac{e_8}{d'_{yz}} & 0 & -\frac{e_{12}}{d'_{zy}} & \frac{e_{11}}{d'_{zy}} \end{bmatrix}^T. \quad (18)$$

Note that Equations (14)–(16) can be used to describe the generalized moments when the beam element has an arbitrary configuration. This can be accomplished by employing coordinate transformations between the global and element local coordinate systems. The following procedure is proposed:

1. The applied moment vector in the global coordinate system, \mathbf{M}_G , is mapped onto the local element coordinate system as follows:

$$\mathbf{M} = \mathbf{J}^{-1}\mathbf{M}_G, \quad (19)$$

where matrix \mathbf{J} can be defined using the slope vectors as follows:

$$\mathbf{J} = \begin{bmatrix} \frac{\partial \mathbf{r}}{\partial x} & \frac{\partial \mathbf{r}}{\partial y} & \frac{\partial \mathbf{r}}{\partial z} \end{bmatrix}. \quad (20)$$

Note that the inverse of the matrix is used instead of the transpose, since the slope vectors do not define an orthogonal frame in a general case.

2. The slope vectors are mapped onto the local element coordinate system as follows:

$$\mathbf{r}'_{,\alpha} = \mathbf{J}^{-1}\mathbf{r}_{,\alpha}, \quad (21)$$

where $\mathbf{r}_{,\alpha} = \partial \mathbf{r}/\partial \alpha$, $\alpha = x, y, z$.

3. The generalized external forces, \mathbf{Q}'_f , associated with the slope vector, $\mathbf{r}'_{,\alpha}$, are calculated using Equations (14)–(16).
4. The external forces associated with the slope vector, $\mathbf{r}'_{,\alpha}$, are mapped to the global coordinate system as follows:

$$\mathbf{Q}_f = \mathbf{J}\mathbf{Q}'_f. \quad (22)$$

In the case of the non-follower moments, matrix \mathbf{J} must be used in mapping. The follower moments can be defined through the use of a constant mapping, \mathbf{J}_0 , which can be defined using initial nodal coordinates and a shape function matrix as follows:

$$\mathbf{J}_0 = \begin{bmatrix} \frac{\partial \mathbf{S}\mathbf{e}_0}{\partial x} & \frac{\partial \mathbf{S}\mathbf{e}_0}{\partial y} & \frac{\partial \mathbf{S}\mathbf{e}_0}{\partial z} \end{bmatrix}. \quad (23)$$

5. The Elastic Forces of a Three-Dimensional Beam Element

A continuum mechanics approach can be used for defining the nonlinear elastic forces of an absolute nodal coordinate beam element [12, 15, 16]. This study discusses the linear and nonlinear expressions for the elastic forces.

5.1. NONLINEAR ELASTIC FORCES

The gradient of the displacement vector can be written as follows:

$$\mathbf{D} = \frac{\partial \mathbf{r}}{\partial \mathbf{x}} \left(\frac{\partial \mathbf{X}}{\partial \mathbf{x}} \right)^{-1} = \frac{\partial (\mathbf{S}\mathbf{e})}{\partial \mathbf{x}} \left[\frac{\partial (\mathbf{S}\mathbf{e}_0)}{\partial \mathbf{x}} \right]^{-1} = \mathbf{J}\mathbf{J}_0^{-1}, \quad (24)$$

where \mathbf{S} is the shape function matrix, \mathbf{X} the vector of the global coordinates, \mathbf{x} the vector of the local element coordinates, and \mathbf{e} and \mathbf{e}_0 are the vectors of the nodal coordinates in the deformed and initial configuration, respectively. Matrix \mathbf{J} is the displacement gradient expressed with respect to the local coordinates, x , y and z . Matrix \mathbf{J}_0 is a constant matrix and must be considered in the formulation of the elastic forces if the element has an arbitrary initial configuration. If the element local coordinate system is parallel to the global coordinate system and the element is not curved, matrix \mathbf{J}_0 is an identity matrix.

The Lagrangian strain tensor, $\boldsymbol{\varepsilon}_m^{nl}$, can be defined using the right Cauchy–Green deformation tensor as follows [10]:

$$\boldsymbol{\varepsilon}_m^{nl} = \frac{1}{2}(\mathbf{D}^T \mathbf{D} - \mathbf{I}), \quad (25)$$

where \mathbf{I} is a 3×3 identity matrix. Because of the symmetry of the strain tensor, it is sufficient to identify only six strain components, ε_{11} , ε_{22} , ε_{33} , ε_{12} , ε_{13} and ε_{23} ; thereby, the strain vector can be written as

$$\boldsymbol{\varepsilon} = [\varepsilon_{11} \ \varepsilon_{22} \ \varepsilon_{33} \ 2\varepsilon_{12} \ 2\varepsilon_{13} \ 2\varepsilon_{23}]^T. \quad (26)$$

The stress components of the element can be defined using the constitutive equation as follows:

$$\boldsymbol{\sigma} = \mathbf{E}\boldsymbol{\varepsilon}, \quad (27)$$

where \mathbf{E} is the matrix of the elastic constants of the material. For an isotropic homogenous material, matrix \mathbf{E} can be expressed in terms of Lamé's constants, λ and μ , as follows:

$$\mathbf{E} = \begin{bmatrix} \lambda + 2\mu & \lambda & \lambda & 0 & 0 & 0 \\ \lambda & \lambda + 2\mu & \lambda & 0 & 0 & 0 \\ \lambda & \lambda & \lambda + 2\mu & 0 & 0 & 0 \\ 0 & 0 & 0 & \mu & 0 & 0 \\ 0 & 0 & 0 & 0 & \mu & 0 \\ 0 & 0 & 0 & 0 & 0 & \mu \end{bmatrix}, \quad (28)$$

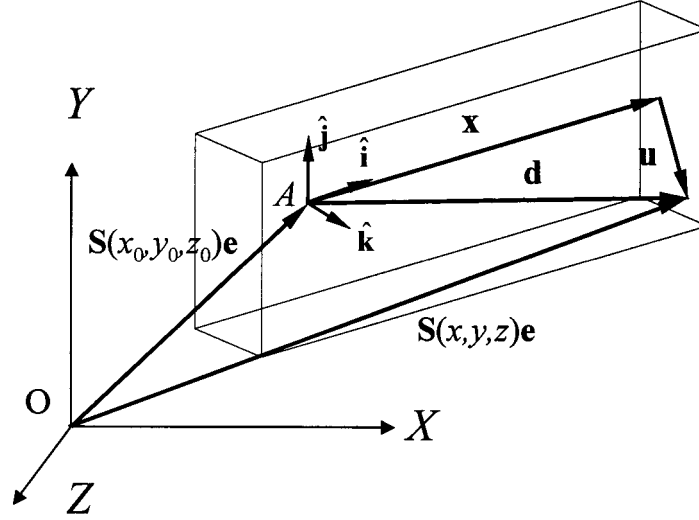


Figure 2. The definition of the vectors in the linear strain-displacement relationship.

where

$$\lambda = \frac{E\nu}{(1+\nu)(1-2\nu)}, \quad \mu = \frac{E}{2(1+\nu)},$$

E is Young's modulus of elasticity and ν is the Poisson ratio of the material.

The elastic forces of the element can be derived by using the following expression of the strain energy:

$$U = \frac{1}{2} \int_V \boldsymbol{\varepsilon}^T \mathbf{E} \boldsymbol{\varepsilon} dV. \quad (29)$$

The vector of the elastic forces, \mathbf{Q}_e , can be defined using the strain energy, U , as follows:

$$\mathbf{Q}_e = \left(\frac{\partial U}{\partial \mathbf{e}} \right)^T. \quad (30)$$

5.2. LINEAR ELASTIC FORCES

In order to define the linear strain-displacement relationship, a local element coordinate system must be used. An orthogonal triad on the element can be defined using the following vectors:

$$\hat{\mathbf{i}} = \frac{\mathbf{r}_x}{|\mathbf{r}_x|}, \quad \hat{\mathbf{k}} = \left(\frac{\mathbf{r}_x}{|\mathbf{r}_x|} \right) \times \left(\frac{\mathbf{r}_y}{|\mathbf{r}_y|} \right), \quad \hat{\mathbf{j}} = \hat{\mathbf{k}} \times \hat{\mathbf{i}}. \quad (31)$$

In the preceding equation, $\mathbf{r}_x = \partial \mathbf{r} / \partial x$ and $\mathbf{r}_y = \partial \mathbf{r} / \partial y$. Figure 2 shows the vectors used in the formulation of the deformation vector. In Figure 2, the displacement vector, \mathbf{d} , is defined as

$$\mathbf{d} = (\mathbf{S}(x, y, z) - \mathbf{S}(x_0, y_0, z_0))\mathbf{e}. \quad (32)$$

Vector \mathbf{d} is defined in the global coordinate system. The deformation vector, \mathbf{u} , in the local element coordinate system can be defined as follows:

$$\mathbf{u} = \mathbf{A}^T \mathbf{d} - \mathbf{x}, \quad (33)$$

where \mathbf{A} is a transformation matrix which can be expressed in terms of unit vectors, $\hat{\mathbf{i}}$, $\hat{\mathbf{j}}$ and $\hat{\mathbf{k}}$, defined in an arbitrary point $A(x_0, y_0, z_0)$,

$$\mathbf{A} = [\hat{\mathbf{i}}_A \ \hat{\mathbf{j}}_A \ \hat{\mathbf{k}}_A]. \quad (34)$$

The displacement gradient can be written as

$$\bar{\mathbf{D}} = \frac{\partial \mathbf{u}}{\partial \mathbf{x}}. \quad (35)$$

The linear strain tensor can be obtained by neglecting the higher-order terms as follows:

$$\boldsymbol{\varepsilon}_m^l \approx \frac{1}{2}(\bar{\mathbf{D}}^T + \bar{\mathbf{D}}). \quad (36)$$

Since the strains are defined in the local coordinate system, they are invariant under arbitrary rigid body motion. The vector of the elastic forces can be calculated using Equations (29) and (30). This model, which is based on the pure continuum mechanics approach, is called Model I.

The continuum mechanics approach is a straightforward method for defining elastic forces. However, in order to achieve accurate results, the finite element should be uniform in all directions, which means that the interpolation functions should be of the same polynomial order in all dimensions. This is not the case in the absolute nodal coordinate beam element. Cubic interpolation is used in the x -direction while linear interpolation is used in the y - and z -directions. For these reasons, the constitutive relations should be modified in order to achieve more accurate results. The problems that can be encountered when using the continuum mechanics approach with inconsistent interpolation are discussed in the section on numerical results.

The strain components that correspond to normal, bending and shear strains can be derived from the linear strain tensor defined in Equation (36). For reasons of simplicity, we assume that the beam element is initially parallel to the global coordinate system. In this case, the transformation matrix, \mathbf{A} , is an identity matrix. The axial strain along the x -axis can be defined as follows:

$$\varepsilon_x^a = S_{1,\xi}e_1 + S_{2,\xi}e_4 + S_{5,\xi}e_{13} + S_{6,\xi}e_{16} - 1, \quad (37)$$

where $S_{i,\xi}$ is the derivative of the shape function, S_i , with respect to ξ . The bending strains can be defined as

$$\varepsilon_x^{\text{bend } Z} = S_{3,\xi}e_7 + S_{7,\xi}e_{19} = \eta(-e_7 + e_{19}), \quad (38)$$

$$\varepsilon_x^{\text{bend } Y} = S_{4,\xi}e_{10} + S_{8,\xi}e_{22} = \eta(-e_{10} + e_{22}). \quad (39)$$

It can be seen that the bending strain is constant along the length of the beam element. Since the cross-section of the beam element can deform, the transverse normal strains are not equal to zero, and they can be calculated as follows:

$$\varepsilon_y = S_{3,\eta}e_8 + S_{7,\eta}e_{20} - 1, \quad (40)$$

$$\varepsilon_z = S_{4,\zeta} e_{12} + S_{8,\zeta} e_{24} - 1. \quad (41)$$

The equations of the transverse shear strains include both constant and linearly varying terms. The constant terms can be written as

$$\gamma_{xy}^V = \frac{1}{2}(S_{1,\xi} e_2 + S_{2,\xi} e_5 + S_{3,\xi} e_7 + S_{5,\xi} e_{14} + S_{6,\xi} e_{17} + S_{7,\xi} e_{19}), \quad (42)$$

$$\gamma_{xz}^V = \frac{1}{2}(S_{1,\xi} e_3 + S_{2,\xi} e_6 + S_{3,\xi} e_{10} + S_{5,\xi} e_{15} + S_{6,\xi} e_{18} + S_{7,\xi} e_{22}). \quad (43)$$

The constant shear strain distribution is known to be inaccurate since the true distribution is parabolic. However, the Timoshenko beam theory assumes the same kind of shear strain distribution, and a shear correction factor is used to obtain the correct shear strain energy. The linearly varying shear strain terms can be written as follows:

$$\gamma_{xy}^T = \frac{1}{2}(S_{4,\xi} e_{11} + S_{8,\xi} e_{23}), \quad (44)$$

$$\gamma_{xz}^T = \frac{1}{2}(S_{3,\xi} e_9 + S_{7,\xi} e_{21}). \quad (45)$$

These shear strains can describe the torsion or distortion of the cross-section. The remaining shear strains are produced by the deformation of the cross-section and can be written as follows:

$$\gamma_{xy}^{\text{def}Y} = \frac{1}{2}(S_{3,\xi} e_8 + S_{7,\xi} e_{20}), \quad (46)$$

$$\gamma_{xz}^{\text{def}Z} = \frac{1}{2}(S_{4,\xi} e_{12} + S_{8,\xi} e_{24}), \quad (47)$$

$$\gamma_{yz} = \frac{1}{2}(S_{3,\eta} e_9 + S_{4,\zeta} e_{11} + S_{7,\zeta} e_{21} + S_{8,\zeta} e_{23}). \quad (48)$$

By employing the above strain definitions, the strain energy of the beam element can be defined as follows:

$$U = \frac{1}{2} \int_0^l \left\{ \sum_{i=1}^5 \Pi_i \right\} dx, \quad (49)$$

where

$$\Pi_1 = EA \{ [(\varepsilon_x^a)^2]_A + [(\varepsilon_y)^2]_A + [(\varepsilon_z)^2]_A \}, \quad (50)$$

$$\Pi_2 = EI_{zz} [(\varepsilon_x^{\text{bend}Z})^2]_A + EI_{yy} [(\varepsilon_x^{\text{bend}Y})^2]_A, \quad (51)$$

$$\Pi_3 = GA \{ k_{sy} [(\gamma_{xy}^V)^2]_A + k_{sz} [(\gamma_{xz}^V)^2]_A \}, \quad (52)$$

$$\Pi_4 = \frac{1}{2} GI_{xx} \{ [(\gamma_{xy}^T)^2]_A + [(\gamma_{xz}^T)^2]_A \}, \quad (53)$$

$$\Pi_5 = GI_{zz}[(\gamma_{xy}^{\text{def}Y})^2]_A + GI_{yy}[(\gamma_{xz}^{\text{def}Z})^2]_A + GA[(\gamma_{yz})^2]_A. \quad (54)$$

In Equations (50–54), A is the area of the cross-section, E and G are the modulus of elasticity and rigidity of the material, respectively, I_{yy} and I_{zz} are the second moments of the area, k_{sy} and k_{sz} are the shear correction factors and I_{xx} is the torsion constant. The brackets with subscript A , $[\cdot]_A$, means that the equation inside is integrated over the area of the cross-section and the resulting area property, i.e. A or $I_{\alpha\alpha}$, is extracted. The strain energy of the beam can also be written as follows:

$$U = \frac{1}{2} \mathbf{e}^T \mathbf{K} \mathbf{e}, \quad (55)$$

where \mathbf{e} is the vector of the nodal coordinates and \mathbf{K} the stiffness matrix, which is given in Appendix A. This model is called Model II. There are three main differences between Model I and Model II:

1. In Model I, the transverse normal strains are coupled using the Poisson ratio. This coupling is removed in Model II. The reason for this is as follows: The transverse normal strains do not depend on the y - and z -coordinates, while the normal strain in the x -direction depends on x , y and z . This means that the following equation is valid only when ε_x is constant with respect to y and z

$$\varepsilon_y(x) = \varepsilon_z(x) = -\nu \varepsilon_x(x, y, z), \quad (56)$$

where $\varepsilon_x(x, y, z) = \varepsilon_x^a + \varepsilon_x^{\text{bend}Z} + \varepsilon_x^{\text{bend}Y}$. In Model I, this leads to spurious results in bending cases.

2. The shear correction factors, k_{sy} and k_{sz} , are used in order to obtain a more accurate value for the shear strain energy.
3. The torsion constant, I_{xx} , is used in Equation (53), since, in general, $I_{xx} \neq I_{yy} + I_{zz}$.

The bending strains in Equations (38) and (39) are constant along the length of the beam, which is different from the classical analytical solution. However, this discrepancy can be corrected by introducing a residual bending flexibility correction. In this method, a fictitious shear parameter, $\bar{\phi}$, is applied such that [9]

$$\frac{1 + \frac{\bar{\phi}}{4}}{\bar{\phi}} = \frac{1 + \frac{\phi}{3}}{\phi}, \quad \bar{\phi} = \frac{\phi}{1 + \frac{\phi}{12}}, \quad \phi = \frac{k_s G A I^2}{E I}. \quad (57)$$

A modified value for the shear correction factor can be calculated as follows:

$$\bar{k}_s = k_s \frac{\bar{\phi}}{\phi}. \quad (58)$$

This beam model, which uses the formulation of Model II, in addition to the residual bending flexibility correction, is called Model III. Note that Models I, II and III can be used for large rotational problems with the use of an incremental solution procedure as explained in Appendix B. It is important to point out that by using generalized description of the strains, the element can be used in the framework of non-incremental solution procedures. This is due to the fact that no assumptions are made with regard to the kinematic motion description of the element.

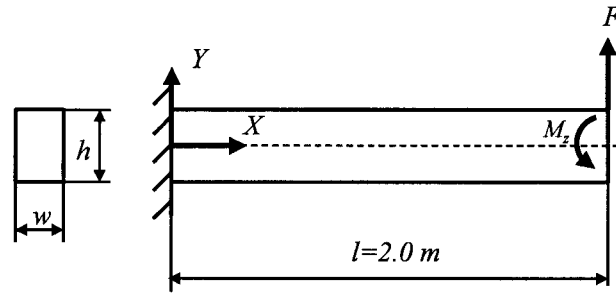


Figure 3. The cantilever beam under investigation in the first four examples.

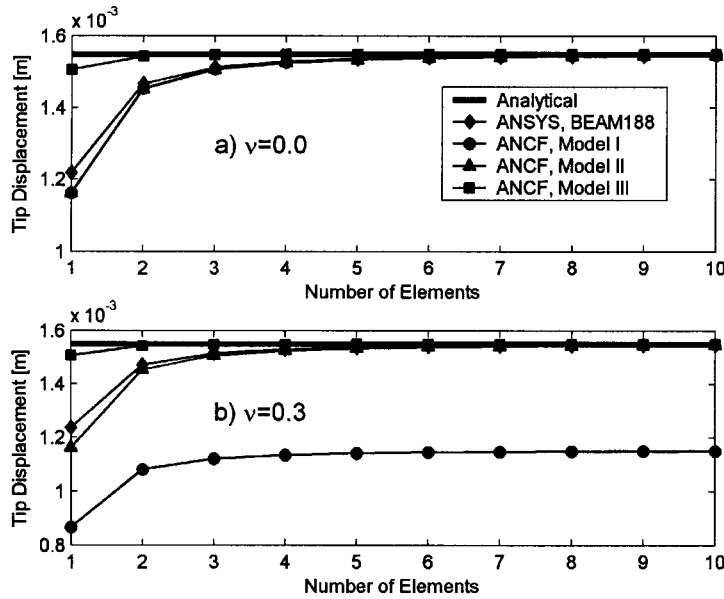


Figure 4. The convergence of the different beam models, (a) a Poisson ratio of 0.0, (b) a Poisson ratio of 0.3.

6. Numerical Examples

This section discusses simple cantilever beam structures. The cantilever beam shown in Figure 3 is considered in the first four examples. One end of the beam is clamped, while forces and moments are applied to the free end. The length of the beam shown in Figure 3 is 2.0 m, and the Young's modulus of the material is $2.07 \cdot 10^{11}$ N/m². Linear deformations are considered in the first three examples, and nonlinear deformations are analyzed in the last two examples.

6.1. CONVERGENCE TEST

In this example, the solution convergence of the different beam models is analyzed. A vertical load, $F = 1,000$ N, is applied to the free end of the cantilever. The cross-section of the beam is a 0.1 m square. The results of the absolute nodal coordinate models (Model I, Model II and Model III) and the ANSYS [14] BEAM188 model are compared with the analytical solution of the cantilever. BEAM188 is a linear beam element based on a formulation proposed by Simo and Vu-Quoc [2] and Ibrahimbegović [6]. The convergence results for the two values of the Poisson ratio, 0.0 and 0.3, are shown in Figure 4. It can be seen in Figure 4 that in the

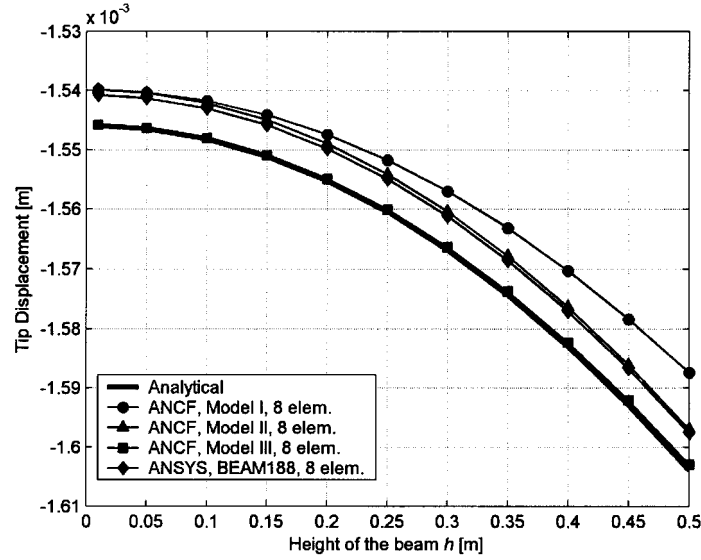


Figure 5. The shear deformation of the cantilever beam.

case of a Poisson ratio of zero, the convergence results of the BEAM188 model and Models I and II are almost equivalent. The best convergence is obtained with Model III that uses the residual bending flexibility correction. When the Poisson ratio of the material is 0.3, the absolute nodal coordinate formulation Model I converges to an inaccurate solution while the other models converge to the analytical solution. This can be explained as follows. A bending load causes an axial normal stress, σ_x , that varies linearly over the cross-section. In Model I, the resulting transverse normal strains can be expressed as follows:

$$\varepsilon_y = \frac{1}{E}[\sigma_y - \nu(\sigma_x + \sigma_z)], \quad \varepsilon_z = \frac{1}{E}[\sigma_z - \nu(\sigma_x + \sigma_y)]. \quad (59)$$

If the cross-section of the beam can deform freely, the transverse normal stresses, σ_y and σ_z , are zero. In bending, the deformed shape of an initially rectangular cross-section is a trapezoid, which is not kinematically possible in the absolute nodal coordinate beam element. As a result, in the case of a bending load, the transverse normal strains are zero, since otherwise, the equilibrium of the finite element solution is not achieved. This, in turn, causes residual transverse normal stresses that contribute to the axial strain as follows:

$$\varepsilon_x = \frac{1}{E}[\sigma_x - \nu(\sigma_y + \sigma_z)]. \quad (60)$$

The result is that Model I predicts overly small displacements.

6.2. SHEAR DEFORMATION IN BENDING

The shear deformation of the cantilever beam is studied in this section. The beam has a rectangular cross-section, the width of which, w , is 0.1 m, and the Poisson ratio of the material is 0.0. The vertical displacement of the end tip of the beam is studied for different values of the height of the beam. The vertical load at the end tip is a function of the height of the beam as follows: $F = -1.0 \cdot 10^6 \cdot h^3$ N. The shear correction factor, k_s , for a rectangular cross-section is $5/6$. In Figures 5 and 6, the vertical displacements of the end tip, which are obtained from the

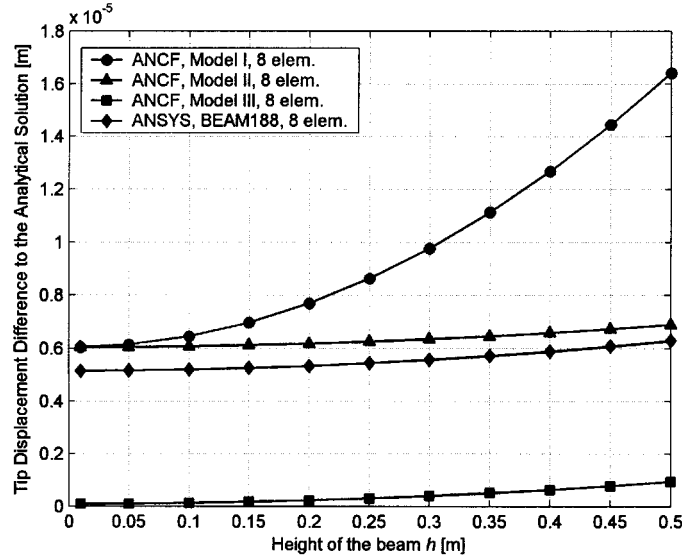


Figure 6. The difference in shear deformation in comparison to the analytical solution of the cantilever beam.

different absolute nodal coordinate beam models and the BEAM188 model, are compared to the analytical solution. It can be seen that the results of the absolute nodal coordinate Model III agree very well with the analytical solution. The results of Model II and the BEAM188 model are almost equivalent while, however, the displacements are underestimated. It is important to note that these elements have a constant bending moment along the length of the beam; therefore, more accurate results can be obtained by increasing the number of elements. The shear deformation predicted by Model I is too small in comparison with the analytical solution. This is simply due to the fact that the shear correction factor is not used in Model I.

6.3. PURE BENDING MOMENT LOAD AND SHEAR DEFORMATION TEST

In this example, a moment load, M_z , is subjected to the end tip of the cantilever beam. The beam is modeled with one element and all the nodal coordinates are fixed in the clamped end. In the case of small linear deformations and after the constraints have been accounted for, the vector of the generalized external forces for the cantilever can be written as

$$\mathbf{Q}_f = [0 \ 0 \ 0 \ 0 \ 0 \ 0 \ -M_z \ 0 \ 0 \ 0 \ 0 \ 0]^T. \quad (61)$$

The unknown nodal displacements of node J can be solved using the following equation:

$$\Delta \mathbf{e}_J = \mathbf{K}_J^{-1} \mathbf{Q}_f, \quad (62)$$

where \mathbf{K}_J is a portion of the stiffness matrix shown in Appendix A. The solution of Equation (62) is

$$\Delta \mathbf{e}_J = \left[0 \ \frac{M_z l^2}{2EI_{zz}} \ 0 \ 0 \ \frac{M_z l}{EI_{zz}} \ 0 \ -\frac{M_z l}{EI_{zz}} \ 0 \ 0 \ 0 \ 0 \ 0 \right]^T. \quad (63)$$

It can be seen that the displacement and rotation of the tip are equal to those given by the beam theory in the analytical solution. By substituting the values of the nodal coordinates into Equation (42), the transverse shear strain can be written as follows:

$$\gamma_{xy}^V = -\frac{3M_z x}{2EI_{zz}} + \frac{3M_z x^2}{2lEI_{zz}} + \frac{M_z x}{EI_{zz}} - \frac{3M_z x^2}{2lEI_{zz}} + \frac{M_z x}{2EI_{zz}} = 0. \quad (64)$$

Under a pure bending moment, the transverse shear strain should be equal to zero. This example implies that the absolute nodal coordinate beam element does not suffer from shear locking.

6.4. NONLINEAR LARGE DEFORMATION EXAMPLES

This section analyzes the nonlinear deformations of two cantilever beams. The results of two different nonlinear absolute nodal coordinate beam models are compared to those obtained with the nonlinear solution (NLGEOM, ON) of the BEAM188 model in ANSYS [14]. The first absolute nodal coordinate beam model uses the nonlinear strain tensor defined in Equation (25). The other model uses the formulation of the elastic forces of linear Model II. Linear Model II can be used in nonlinear deformation analysis by employing an updating procedure, which is described in Appendix B. The nonlinear equations are solved using the Newton–Raphson iteration procedure in which the values of the nodal coordinates can be calculated at step $n + 1$ as follows:

$$\mathbf{e}^{(n+1)} = \mathbf{e}^{(n)} - (\mathbf{K}_T^{(n)})^{-1} \mathbf{Q}^{(n)}, \quad (65)$$

where $\mathbf{K}_T^{(n)}$ is the tangent stiffness matrix and vector $\mathbf{Q}^{(n)}$ includes the elastic and external forces at iteration step n as follows:

$$\mathbf{Q}^{(n)} = \mathbf{Q}_e^{(n)} - \mathbf{Q}_f^{(n)}. \quad (66)$$

In the absolute nodal coordinate formulation, the tangent stiffness matrix can be written as

$$\mathbf{K}_T^{(n)} = \frac{\partial \mathbf{Q}^{(n)}}{\partial \mathbf{e}^{(n)}}. \quad (67)$$

In the solution process, the tangent stiffness matrix is calculated numerically using perturbations in the nodal coordinates and finite differences. The convergence criterion for the iteration is defined as follows:

$$|\mathbf{Q}| < 0.001 \cdot |\mathbf{Q}_f|, \quad (68)$$

where $|\cdot|$ is the Euclidean norm of the vector.

6.4.1. Tip-Loaded Cantilever

Two cases of the cantilever shown in Figure 3 are analyzed in this section. In Case I, the beam has a 0.1 m square cross-section and the Poisson ratio of the material is 0.3. In Case II, the Poisson ratio is 0.0 and the width and the height of the beam are 0.1 and 0.5 m, respectively. The vertical force, F , at the free end of the beam is $-5.0 \cdot 10^8 \cdot h^3$ N in both cases. The positions of the end tip obtained using different models and different numbers of elements are shown in Tables 1 and 2. In Case I (Table 1), the nonlinear absolute nodal coordinate model predicts smaller deformations than do the other models. This is caused by the non-zero Poisson ratio,

Table 1. The beam end tip positions in Case I.

Number of elements	Tip Position (X, Y), [m]		
	ANCF Linear Model II	BEAM188	ANCF Nonlinear
2	1.95300, -0.39046	1.87080, -0.65671	1.95536, -0.37731
4	1.88691, -0.60210	1.85918, -0.67485	1.91969, -0.50935
8	1.85901, -0.67235	1.85618, -0.67947	1.91342, -0.53039
16	1.85570, -0.67995	1.85540, -0.68069	1.91274, -0.53271
32	1.85530, -0.68077	1.85520, -0.68100	1.91262, -0.53313
64	1.85523, -0.68091	1.85515, -0.68108	1.91259, -0.53323

Table 2. The beam end tip positions in Case II.

Number of elements	Tip Position (X, Y), [m]		
	ANCF Linear Model II	BEAM188	ANCF Nonlinear
2	1.88585, -0.62403	1.86749, -0.67783	1.86888, -0.64147
4	1.85680, -0.69233	1.85551, -0.69700	1.84807, -0.69512
8	1.85192, -0.70278	1.85246, -0.70179	1.84462, -0.70421
16	1.85089, -0.70494	1.85169, -0.70299	1.84371, -0.70654
32	1.85063, -0.70551	1.85150, -0.70329	1.84341, -0.70725
64	1.85057, -0.70569	1.85145, -0.70337	1.84330, -0.70750

which results in residual transverse normal stresses in the element, as explained in Section 6.1. Linear Model II and the BEAM188 model converge to equivalent solutions as the number of elements is increased. In Case II (Table 2), the discrepancies between the different models are not as large as in Case I; however, both ANCF models predict slightly larger deformations than does the BEAM188 model.

6.4.2. General Moment Load

In this section, the cantilever beam, shown in Figure 7, is analyzed. The clamped end of the beam is at point (0.0 m, 0.0 m, 0.0 m), while the free end is at point (2.0 m, 1.0 m, 0.5 m). The cross-section of the beam is a 0.1 m square and the Poisson ratio of the material is 0.0. The beam is modeled using eight elements. A moment load, M_X , about the global X-axis is applied to the free end. Table 3 shows the deformations of the end tip obtained using different models and different values of moment M_X . The results of the nonlinear absolute nodal coordinate model and the BEAM188 model are in good agreement, while the linear ANCF model predicts larger deformations when the applied moment is large. In this particular example, the nonlinear ANCF model gives good results, since the Poisson ratio is zero and transverse shear deformation is zero. On the other hand, the accuracy of the linear model decreases when the deformations are large. In [17] it was shown that the linear model gives correct results in the case of a small torsion load. It must be noted that ANSYS could not find the solution when $M_X = 1.0 \cdot 10^6$ Nm, while no convergence problems were encountered with the ANCF models.

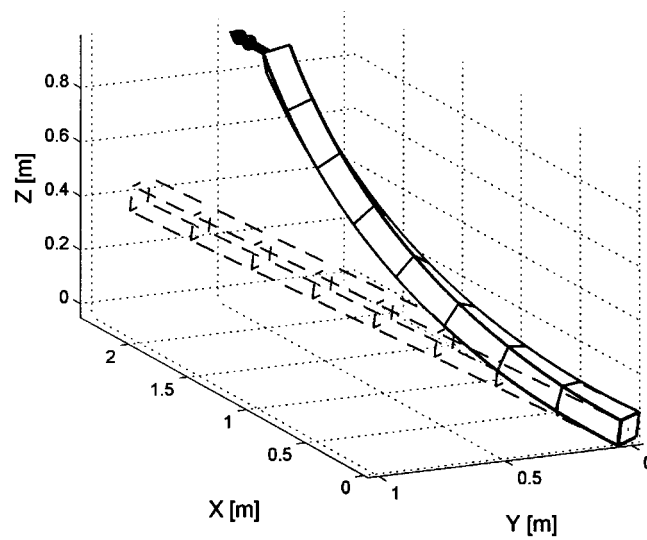


Figure 7. The deformed shape of the beam obtained with the non-linear ANCF model and with a moment load, M_X , of $1.0 \cdot 10^6$ Nm.

Table 3. The beam end tip positions in the case of the moment load.

Moment M_X [Nm]	Deformation at end tip UX, UY, UZ [m]		
	ANCF Linear Model II	ANCF Nonlinear	BEAM188
$1.0 \cdot 10^4$	-0.00002, -0.00332, 0.00664	-0.00000, -0.00335, 0.00663	-0.00000, -0.00335, 0.00663
$5.0 \cdot 10^4$	-0.00048, -0.01659, 0.03325	-0.00000, -0.01658, 0.03325	-0.00000, -0.01733, 0.03283
$1.0 \cdot 10^5$	-0.00191, -0.03319, 0.06667	-0.00001, -0.03608, 0.06485	-0.00001, -0.03608, 0.06486
$5.0 \cdot 10^5$	-0.05121, -0.18306, 0.35461	-0.00042, -0.23082, 0.28369	-0.00071, -0.23164, 0.28442
$1.0 \cdot 10^6$	-0.21699, -0.55726, 0.74477	-0.00225, -0.54704, 0.43791	no solution

7. Conclusions

This investigation compared different elastic force models of the absolute nodal coordinate formulation for a three-dimensional beam element. A straightforward procedure can be obtained for elastic forces by employing the continuum mechanics approach. In the three-dimensional beam element, the interpolation polynomials are cubic in the axial direction and linear in the cross-sectional direction. For this reason, the pure continuum mechanics approach should be used with care when deriving the elastic forces. This study showed that the accuracy of elastic forces based on continuum mechanics can be improved by modifying the constitutive relations. The proposed improvement to the elastic forces can describe transverse shear deformation more accurately and was verified using several numerical examples. The numerical examples demonstrate that the proposed elastic force model of the beam element agrees with the analytical results as well as with solutions obtained using existing finite element formulation.

Most finite element formulation that takes transverse shear deformation into account suffers from shear locking caused by the tendency of the element to store excess shear strain energy. The numerical results for the beam element under investigation imply that the absolute nodal coordinate formulation for the beam element does not suffer from shear locking. In the three-dimensional beam element, global displacements and slopes are used as the nodal coordinates, which results in a large number of nodal degrees of freedom. This study gives a physical interpretation of the nodal coordinates used in the absolute nodal coordinate beam element. This study also introduced descriptions for the generalized external moments in a three-dimensional case. It has been shown that a beam element based on the absolute nodal coordinate formulation relaxes the assumption of a rigid cross-section and is capable of representing the distortional deformation of the cross-section.

Appendix A

The linear stiffness matrix of the absolute nodal coordinate beam element (Models II and III) can be written as

$$\mathbf{K} = \begin{bmatrix} \mathbf{K}_{11} & \mathbf{K}_{12} & \mathbf{K}_{13} & \mathbf{K}_{14} \\ & \mathbf{K}_{22} & \mathbf{K}_{23} & \mathbf{K}_{24} \\ & & \mathbf{K}_{33} & \mathbf{K}_{34} \\ \text{symm.} & & & \mathbf{K}_{44} \end{bmatrix}, \quad (\text{A.1})$$

where \mathbf{K}_{ij} are 6×6 matrices, the non-zero elements of which are as follows:

$$\mathbf{K}_{11}(1, 1) = -\mathbf{K}_{13}(1, 1) = \mathbf{K}_{33}(1, 1) = \frac{6}{5} \frac{EA}{L},$$

$$\mathbf{K}_{11}(2, 2) = -\mathbf{K}_{13}(2, 2) = \mathbf{K}_{33}(2, 2) = \frac{6}{5} \frac{k_{sy}GA}{L},$$

$$\mathbf{K}_{11}(3, 3) = -\mathbf{K}_{13}(3, 3) = \mathbf{K}_{33}(3, 3) = \frac{6}{5} \frac{k_{sz}GA}{L},$$

$$\mathbf{K}_{11}(4, 4) = -4\mathbf{K}_{13}(4, 4) = \mathbf{K}_{33}(4, 4) = \frac{2}{15} EAL,$$

$$\mathbf{K}_{11}(5, 5) = -4\mathbf{K}_{13}(5, 5) = \mathbf{K}_{33}(5, 5) = \frac{2}{15}k_{sy}GAL,$$

$$\mathbf{K}_{11}(6, 6) = -4\mathbf{K}_{13}(6, 6) = \mathbf{K}_{33}(6, 6) = \frac{2}{15}k_{sz}GAL,$$

$$\begin{aligned}\mathbf{K}_{11}(1, 4) &= \mathbf{K}_{11}(4, 1) = \mathbf{K}_{13}(1, 4) = -\mathbf{K}_{13}(4, 1) = -\mathbf{K}_{33}(1, 4) \\ &= -\mathbf{K}_{33}(4, 1) = \frac{1}{10}EAL,\end{aligned}$$

$$\begin{aligned}\mathbf{K}_{11}(2, 5) &= \mathbf{K}_{11}(5, 2) = \mathbf{K}_{13}(2, 5) = -\mathbf{K}_{13}(5, 2) = -\mathbf{K}_{33}(2, 5) \\ &= -\mathbf{K}_{33}(5, 2) = \frac{1}{10}k_{sy}GAL,\end{aligned}$$

$$\begin{aligned}\mathbf{K}_{11}(3, 6) &= \mathbf{K}_{11}(6, 3) = \mathbf{K}_{13}(3, 6) = -\mathbf{K}_{13}(6, 3) = -\mathbf{K}_{33}(3, 6) \\ &= -\mathbf{K}_{33}(6, 3) = \frac{1}{10}k_{sz}GAL,\end{aligned}$$

$$\mathbf{K}_{12}(2, 1) = \mathbf{K}_{14}(2, 1) = -\mathbf{K}_{23}(1, 2) - \mathbf{K}_{34}(2, 1) = -\frac{1}{2}k_{sy}GA,$$

$$\mathbf{K}_{12}(3, 4) = \mathbf{K}_{14}(3, 4) = -\mathbf{K}_{23}(4, 3) = -\mathbf{K}_{34}(3, 4) = -\frac{1}{2}k_{sz}GA,$$

$$\mathbf{K}_{12}(5, 1) = -\mathbf{K}_{14}(5, 1) = -\mathbf{K}_{23}(1, 5) = \mathbf{K}_{34}(5, 1) = \frac{1}{12}k_{sy}GAL,$$

$$\mathbf{K}_{12}(6, 4) = -\mathbf{K}_{14}(6, 4) = -\mathbf{K}_{23}(4, 6) = \mathbf{K}_{34}(6, 4) = \frac{1}{12}k_{sz}GAL,$$

$$\mathbf{K}_{22}(1, 1) = \mathbf{K}_{44}(1, 1) = \frac{k_{sy}GAL}{3} + \frac{EI_{zz}}{L},$$

$$\mathbf{K}_{22}(2, 2) = \mathbf{K}_{44}(2, 2) = \frac{EAL}{3} + \frac{GI_{zz}}{L},$$

$$\mathbf{K}_{22}(3, 3) = \mathbf{K}_{44}(3, 3) = \mathbf{K}_{22}(5, 5) = \mathbf{K}_{44}(5, 5) = \frac{GAL}{3} + \frac{GI_{xx}}{2L},$$

$$\mathbf{K}_{22}(4, 4) = \mathbf{K}_{44}(4, 4) = \frac{k_{sz}GAL}{3} + \frac{EI_{yy}}{L},$$

$$\mathbf{K}_{22}(6, 6) = \mathbf{K}_{44}(6, 6) = \frac{EAL}{3} + \frac{GI_{yy}}{L},$$

$$\mathbf{K}_{22}(3, 5) = \mathbf{K}_{44}(3, 5) = \mathbf{K}_{22}(5, 3) = \mathbf{K}_{44}(5, 3) = \frac{GAL}{3},$$

$$\mathbf{K}_{24}(1, 1) = \frac{k_{sy}GAL}{6} - \frac{EI_{zz}}{L},$$

$$\mathbf{K}_{24}(2, 2) = \frac{EAL}{6} - \frac{GI_{zz}}{L},$$

$$\mathbf{K}_{24}(3, 3) = \mathbf{K}_{24}(5, 5) = \frac{GAL}{6} - \frac{GI_{xx}}{2L},$$

$$\mathbf{K}_{24}(4, 4) = \frac{k_{sz}GAL}{6} - \frac{EI_{yy}}{L},$$

$$\mathbf{K}_{24}(6, 6) = \frac{EAL}{6} - \frac{GI_{yy}}{L}.$$

Appendix B. The Updating Procedure for the Linear Model II

The following steps are performed in the updating procedure:

1. The transformation matrix, \mathbf{A} , is calculated at point $(x_0, y_0, z_0) = (l/2, 0, 0)$ on the element using the nodal coordinates of iteration step n . Matrix \mathbf{A} is used in the definition of the 24×24 transformation matrix, \mathbf{T} , as follows:

$$\mathbf{T} = \begin{bmatrix} \mathbf{A} & \mathbf{0} & \mathbf{0} & \mathbf{0} & \mathbf{0} & \mathbf{0} & \mathbf{0} & \mathbf{0} & \mathbf{0} \\ \mathbf{0} & \mathbf{A} & \mathbf{0} & \mathbf{0} & \mathbf{0} & \mathbf{0} & \mathbf{0} & \mathbf{0} & \mathbf{0} \\ \mathbf{0} & \mathbf{0} & \mathbf{A} & \mathbf{0} & \mathbf{0} & \mathbf{0} & \mathbf{0} & \mathbf{0} & \mathbf{0} \\ \mathbf{0} & \mathbf{0} & \mathbf{0} & \mathbf{A} & \mathbf{0} & \mathbf{0} & \mathbf{0} & \mathbf{0} & \mathbf{0} \\ \mathbf{0} & \mathbf{0} & \mathbf{0} & \mathbf{0} & \mathbf{A} & \mathbf{0} & \mathbf{0} & \mathbf{0} & \mathbf{0} \\ \mathbf{0} & \mathbf{0} & \mathbf{0} & \mathbf{0} & \mathbf{0} & \mathbf{A} & \mathbf{0} & \mathbf{0} & \mathbf{0} \\ \mathbf{0} & \mathbf{0} & \mathbf{0} & \mathbf{0} & \mathbf{0} & \mathbf{0} & \mathbf{A} & \mathbf{0} & \mathbf{0} \\ \mathbf{0} & \mathbf{0} & \mathbf{0} & \mathbf{0} & \mathbf{0} & \mathbf{0} & \mathbf{0} & \mathbf{A} & \mathbf{0} \\ \mathbf{0} & \mathbf{0} & \mathbf{0} & \mathbf{0} & \mathbf{0} & \mathbf{0} & \mathbf{0} & \mathbf{0} & \mathbf{A} \end{bmatrix}, \quad (\text{B.1})$$

where $\mathbf{0}$ is a 3×3 null matrix.

2. The nodal coordinates are transformed into the initial reference coordinate system, because in linear Models I, II and III the strains are defined in the initial reference coordinate system. The relation can be expressed as follows:

$$\bar{\mathbf{e}}^{(n)} = \mathbf{T}^T \mathbf{e}^{(n)}, \quad (\text{B.2})$$

3. The vector of the elastic forces, $\bar{\mathbf{Q}}_e^{(n)}$, is calculated using the nodal coordinate vector, $\bar{\mathbf{e}}^{(n)}$.
4. The vector of the elastic forces, $\bar{\mathbf{Q}}_e^{(n)}$, is transformed into the global coordinate system as follows:

$$\mathbf{Q}_e^{(n)} = \mathbf{T} \bar{\mathbf{Q}}_e^{(n)}. \quad (\text{B.3})$$

5. The calculation of $\mathbf{Q}^{(n)}$, the tangent stiffness matrix, $\mathbf{K}_T^{(n)}$, and the solution of the nodal coordinates at iteration step $n + 1$.
6. Return to step 1.

The above-presented updating procedure allows for the incremental solution of linear absolute nodal coordinate formulation elements.

References

1. Simo, J. C., 'A finite strain beam formulation. The three-dimensional dynamic problem. Part I', *Computer Methods in Applied Mechanics and Engineering* **49**, 1985, 55–70.
2. Simo, J. C. and Vu-Quoc, L., 'A three-dimensional finite-strain rod model. Part II: Computational aspects', *Computer Methods in Applied Mechanics and Engineering* **58**, 1986, 79–116.
3. Cardona, A. and Geradin, M., 'A beam finite element non-linear theory with finite rotations', *International Journal for Numerical Methods in Engineering* **26**, 1988, 2403–2438.
4. Avello, A. and García de Jalón, J., 'Dynamics of flexible multibody systems using Cartesian coordinates and large displacement theory', *International Journal for Numerical Methods in Engineering* **32**, 1991, 1543–1563.
5. Jelenić, G. and Saje, M., 'A kinematically exact space finite strain beam model – Finite element formulation by generalized virtual work principle', *Computer Methods in Applied Mechanics and Engineering* **120**, 1995, 131–161.
6. Ibrahimbegović, A., 'On the finite element implementation of geometrically nonlinear Reissner's beam theory: Three-dimensional curved beam elements', *Computer Methods in Applied Mechanics and Engineering* **122**, 1995, 11–26.
7. Jelenić, G. and Crisfield, M. A., 'Interpolation of rotational variables in nonlinear dynamics of 3D beams', *International Journal for Numerical Methods in Engineering* **43**, 1998, 1193–1222.
8. Jelenić, G. and Crisfield, M. A., 'Geometrically exact 3D beam theory: Implementation of a strain-invariant finite elements for statics and dynamics', *Computer Methods in Applied Mechanics and Engineering* **171**, 1999, 141–171.
9. Géradin, M. and Cardona, A., *Flexible Multibody Dynamics: A Finite Element Approach*, Wiley, West Sussex, 2001.
10. Shabana, A. A., *Dynamics of Multibody Systems*, Wiley, New York, 1998.
11. Shabana, A. A. and Yakoub, R. Y., 'Three dimensional absolute nodal coordinate formulation for beam elements: Theory', *ASME Journal of Mechanical Design* **123**, 2001, 606–613.
12. Yakoub, R. Y. and Shabana, A. A., 'Three dimensional absolute nodal coordinate formulation for beam elements: Implementation and application', *ASME Journal of Mechanical Design* **123**, 2001, 614–621.
13. Mikkola, A. M. and Shabana, A. A., 'A new plate element based on the absolute nodal coordinate formulation', in *Proceedings of DETC'01, ASME Design Engineering Technical Conferences and Computers and Information in Engineering Conference*, Pittsburgh, PA, September 9–12, 2001.
14. ANSYS User's Manual, Theory, Twelfth Edition, SAS IP Inc., 2001.
15. Berzeri, M. and Shabana, A. A., 'Development of simple models for the elastic forces in the absolute nodal coordinate formulation', *Journal of Sound and Vibration* **235**, 2000, 539–565.
16. Omar, M. A. and Shabana, A. A., 'A two-dimensional shear deformation beam for large rotation and deformation', *Journal of Sound and Vibration* **243**(3), 2001, 565–576.
17. Sopanen, J. T. and Mikkola, A. M., 'Studies on the stiffness properties of the absolute nodal coordinate formulation for three-dimensional beams', in *Proceedings of DETC'03, ASME Design Engineering Technical Conferences and Computers and Information in Engineering Conference*, Chicago, IL, 2003, DETC2003/VIB-48325.